

# Explainability Methods for Hardware Trojan Detection: A Systematic Comparison

Paul Whitten<sup>1\*</sup>, Francis Wolff<sup>1†</sup> and Chris Papachristou<sup>1†</sup>

<sup>1</sup>\*Electrical, Computer, and Systems Engineering, Case Western Reserve University, 10900 Euclid Avenue, Cleveland, 44106, State, USA.

\*Corresponding author(s). E-mail(s): [pcw@case.edu](mailto:pcw@case.edu);

Contributing authors: [fxw12@case.edu](mailto:fxw12@case.edu); [cap2@case.edu](mailto:cap2@case.edu);

†These authors contributed equally to this work.

## Abstract

Hardware trojan detection requires both accurate identification and interpretable explanations that enable hardware security engineers to understand and act on detection results. While machine learning approaches show promise, existing explainability methods developed for general domains like image classification may not provide the actionable insights that hardware engineers need. A question remains: How do domain-aware property analysis, model-agnostic case-based reasoning, and model-agnostic feature attribution techniques compare for hardware security applications?

This work compares three categories of explainability for gate-level hardware trojan detection on the Trust-Hub benchmark dataset: (1) domain-aware property-based analysis of 31 circuit-specific features derived from gate fanin patterns, flip-flop distances, and primary I/O connectivity; (2) model-agnostic case-based reasoning using k-nearest neighbors for precedent-based explanations; and (3) model-agnostic feature attribution methods (LIME, SHAP, gradient) that provide generic importance scores without circuit-level context.

The findings show that different explainability approaches offer distinct advantages for hardware security practitioners. The domain-aware property-based method analyzes 31 circuit properties, enabling engineers to understand detection decisions through familiar concepts like "high fanin complexity near outputs indicates potential trojan triggers." Case-based reasoning (k-nearest neighbors) achieves 97.4% correspondence between predictions and training exemplars, providing model-agnostic justifications grounded in precedent that require minimal domain interpretation. In contrast, while LIME and SHAP provide mathematically rigorous feature attributions with strong inter-method correlation ( $\rho=0.94$ ,  $p<0.001$ ), they produce generic feature importance scores that lack circuit-level

context for validation or remediation planning. Detection performance using XGBoost classification with optimized threshold achieves 46.15% precision and 52.17% recall on 11,392 test samples, representing a 9-fold improvement over prior work (Hasegawa et al.: 5.13% precision) while reducing false positive rates from approximately 5.6% to 0.25%.

Additionally, gradient-based feature attribution (Simonyan et al., 2013), while 481 times faster than SHAP, provides similar domain-opaque insights as other model-agnostic methods, confirming that computational efficiency alone cannot substitute for domain-aware interpretability.

This work provides empirical evidence comparing domain-aware property analysis, model-agnostic case-based reasoning, and model-agnostic feature attribution techniques for hardware security applications. The results show that property-based and case-based approaches offer complementary advantages: domain alignment and precedent-based interpretability, respectively, compared to generic feature rankings. These findings have implications for XAI deployment across domains where practitioners must validate and act on ML predictions.

**Keywords:** explainable artificial intelligence, hardware trojan detection, domain-aware explainability, model-agnostic explanations, circuit property analysis, LIME, SHAP, XGBoost, Trust-Hub benchmark

## 1 Introduction

When a machine learning system flags a gate in a billion-transistor integrated circuit as a potential hardware trojan, what should the security engineer do next? Generic explanations like "feature importance: 0.73" provide little guidance for validating the detection or planning remediation. This explainability gap represents a barrier to deploying ML-based trojan detection in practice: without actionable interpretations grounded in circuit design principles, engineers cannot distinguish meaningful alerts from false positives, cannot verify suspicious structural patterns against domain knowledge, and cannot translate detection results into concrete security actions.

Hardware trojans are malicious circuit modifications introduced during design or fabrication that pose unique challenges compared to software vulnerabilities. Unlike software patches, hardware trojans are permanent components of silicon. Unlike software bugs triggered by common code paths, hardware trojans activate through rare input combinations designed to evade conventional testing (as few as 1 in  $2^{64}$  possible states). Unlike software exploits visible through runtime monitoring, hardware trojans operate at the gate-level where they can compromise system confidentiality, integrity, or availability with no software-visible trace. As infrastructure, financial systems, and defense applications depend on integrated circuits fabricated through complex global supply chains involving potentially untrusted facilities, hardware trojan detection capabilities have become important for supply chain security and system integrity.

Machine learning approaches have demonstrated promise for hardware trojan detection by identifying suspicious circuit structures through statistical analysis of

gate-level netlists. However, existing ML-based detection methods face a challenge: opaque-box models provide predictions without interpretable justifications that hardware security engineers can understand and act upon. While explainable AI (XAI) techniques have been developed to interpret ML predictions, these methods were primarily designed for general domains like image classification and natural language processing. This raises the question: *Do model-agnostic explainability techniques developed for general ML applications provide the actionable insights that hardware security practitioners need, or do domain-aware methods tailored to circuit characteristics offer interpretability?*

Explainability is important in hardware trojan detection because security engineers need actionable insights: not just feature importance scores, but interpretations grounded in circuit design principles that enable validation and remediation. When a detection system flags a gate as suspicious, engineers need to understand the finding in terms they can verify: "This gate exhibits high fanin complexity (12 inputs at 2 levels) near a primary output, matching the signature of trojan trigger circuits." Generic explanations like "feature X has importance 0.73" provide limited actionability for domain experts.

This distinction between domain-aware and model-agnostic explainability represents a tradeoff in XAI system design. Model-agnostic methods like LIME [1] and SHAP [2] offer mathematical rigor and applicability across any ML model, explaining predictions through feature perturbation and game-theoretic attribution. These methods have been applied effectively to image classification and text analysis where generic feature importance suffices. However, in specialized domains like hardware security, model-agnostic methods may lack the domain context necessary for practitioners to trust and act on explanations.

Domain-aware explainability methods, in contrast, incorporate domain knowledge directly into the explanation framework. For hardware trojan detection, this means analyzing circuit-specific properties like gate fanin patterns, flip-flop connectivity, and proximity to primary I/O, characteristics that hardware engineers routinely use to reason about circuit behavior. While domain-aware methods require domain expertise to design, they align with existing practitioner knowledge and reasoning patterns. Yet prior work has not empirically evaluated whether this theoretical advantage translates to practical benefits for hardware security applications.

This work provides an empirical comparison of domain-aware versus model-agnostic explainability methods for hardware trojan detection. The evaluation focuses on whether domain-specific circuit property analysis provides more actionable insights compared to general-purpose feature attribution techniques (LIME, SHAP) when applied to gate-level netlist analysis on the Trust-Hub benchmark dataset.

The primary contributions are:

1. **Domain-Aware Property Analysis:** A property-based explainability method is developed and evaluated that analyzes 31 circuit-specific features grounded in hardware design principles. This domain-aware approach provides explanations like "high Logic Gate Fanin (LGF<sub>i</sub>=12) at 2 levels upstream combined with low Flip-Flop Output distance (ffo=1) matches rare-event trigger patterns," enabling hardware engineers to validate findings through familiar circuit analysis concepts.

2. **Case-Based Reasoning with k-Nearest Neighbors:** An inherently interpretable prediction method using k-nearest neighbors (k=5) achieves 97.4% correspondence between predictions and training exemplars. This approach provides justifications grounded in precedent: "This gate's feature profile matches 4 out of 5 similar training cases that were trojans," enabling engineers to validate detections through comparison with known patterns.
3. **Comparison with Model-Agnostic Baselines:** Domain-aware and inherently interpretable methods are compared against model-agnostic techniques (LIME, SHAP) that provide generic feature importance without circuit-level context. While LIME and SHAP exhibit strong inter-method correlation ( $\rho=0.94$ ,  $p<0.001$ ) validating their mathematical consistency, generic feature rankings provide limited actionability for hardware security practitioners. Gradient-based attribution (Simonyan et al., 2013) is also evaluated for computational efficiency.
4. **Improved Detection Performance with XGBoost:** The XGBoost-based detector achieves 46.15% precision (95% CI: [42.06%, 50.24%]) at 52.17% recall (95% CI: [45.65%, 58.70%]) on Trust-Hub circuits, representing a 9-fold improvement in precision over the Hasegawa et al. baseline (5.13% precision, 82.6% recall). This improvement addresses a key limitation for practical deployment where engineers must investigate flagged gates.

Section 2 provides background on hardware trojans and explainable AI techniques. Section 3 reviews related work in ML-based trojan detection. Sections 4 and 5 describe the methodology and experimental setup. Section 6 presents results and Section 7 discusses implications and future work.

## 2 Background

### 2.1 Hardware Trojans

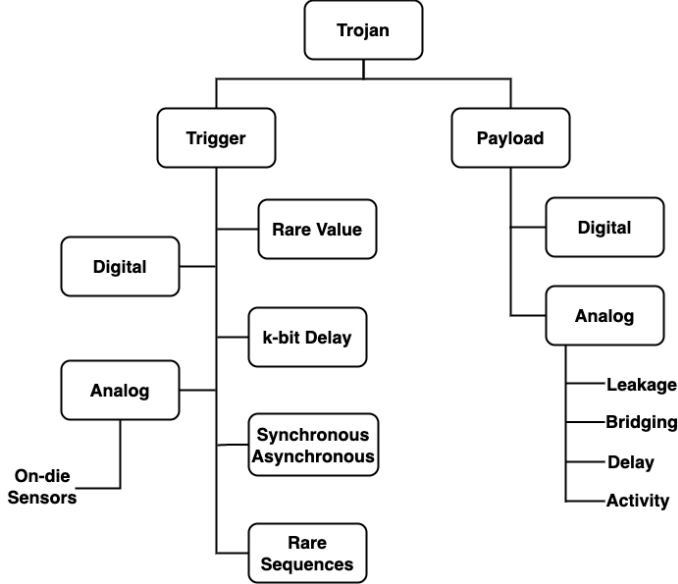


**Fig. 1:** Trojan circuit taxonomy[3].

Cost-reducing measures in the semiconductor manufacturing industry have led to outsourcing integrated circuit processes. Outsourcing presents a security risk due to the increased potential for insertion of hardware trojans into trusted integrated circuits. Hardware trojans are injected by attackers to weaken the confidentiality, integrity, or availability of an integrated circuit.

A hardware trojan circuit taxonomy is shown in Figure 1. A hardware trojan circuit has two primary parts: the trigger, which activates the trojan, and the payload, which delivers the exploit. Triggers may be classified as digital or analog. Off-die sensors may trigger analog triggers. Rare values, k-bit synchronous or asynchronous delays, and rare sequences may activate triggers. Payloads may also be digital or analog. Digital payloads could alter control, status, or data lines. Analog payloads could exploit the circuit by introducing leakage, bridging, delay, or unintended activity[3].

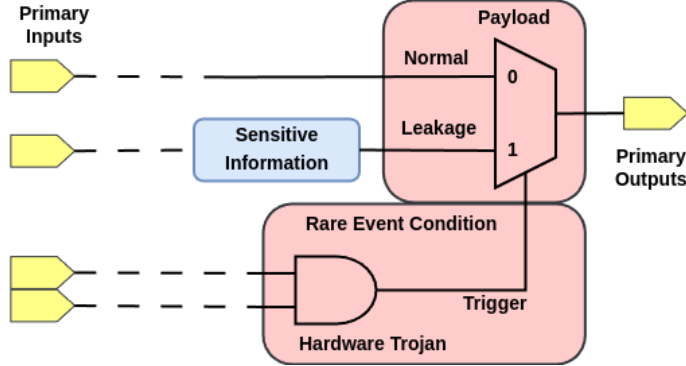


**Fig. 2:** Confidentiality rare event hardware trojan model.

Figure 2 shows a specific implementation of a confidentiality hardware trojan using logic gates within an IC design file netlist. The dashed lines represent additional levels of logic gates. The trigger is conditional on input patterns within the IC, which eventually originate from the primary inputs. The logical-and gate requires that all the inputs are logically true before triggering the payload. To be difficult to detect or accidentally trigger during IC test mode, the hardware trojan trigger should be a rare event condition. Given  $n$  inputs to a combinational IP circuit, the rarest condition would be one of  $2^n$  inputs. Once the hardware trojan is triggered, the multiplexor circuit within the payload switches from normal operation to leaking sensitive information on the primary output pin of the circuit where the attacker can observe it.

This rare event hardware trojan model allows for detection through static circuit analysis by examining each net or group of logic gates within an IP circuit primary for input or fanin complexity. The greater the fanin, the higher the probability that a subcircuit is a potential suspect for a hardware trojan. Additionally, payloads must propagate their sensitive information to the primary output. The rare event fanin and primary output payload concepts form the basis of trojan analysis of several methodologies [3–6].

Fanin and output payload are features of a net or set of logic gates. Features are used widely in ML classification and pattern recognition. Individual features may contribute little to identification. The combination of features, however, is useful for effective classification and can also explain a system's results.

Hasegawa et al. introduced a method of detecting hardware trojans from a gate-level netlist [4, 5]. Five features from each net are used to classify trojans. (a) Logic Gate Fanins (LGF<sub>i</sub>) represent the number of inputs to the logic gates two levels upstream from a net. (b) Flip-Flop Input (FF<sub>i</sub>) represents the number of upstream logic levels to a flip-flop. (c) Flip-Flop Output (FF<sub>o</sub>) represents the number of logic levels downstream to a flip-flop. (d) Primary Input (PI) which represents the number of logic levels upstream to the closest primary input. (e) Primary Output (PO) represents the number of logic levels downstream to the closest primary output. In the work, the authors also used three training strategies, due to the imbalance of the trojan to non-trojan training data ratio: no weighting, static weighting, and dynamic

weighting. Dynamic weighting performed best. Other works address the imbalance in other means, such as synthetic method over-sampling techniques [7]. These optimized methods still do not provide a better understanding of the ML results.

## 2.2 Trust-Hub Trojan Database

The Trust-Hub benchmark repository [6, 8–10] provides gate-level netlists with known trojan insertions for various circuit types. This work uses 30 circuits comprising RS232 communication peripherals and ISCAS combinational benchmarks.

# 3 Related Work

## 3.1 Machine Learning for Hardware Trojan Detection

### 3.1.1 Hasegawa et al. Baseline

Hasegawa et al. established a foundational approach for ML-based hardware trojan detection from gate-level netlists [4, 5]. Their method extracts five structural features from each net: Logic Gate Fanins (LGF<sub>i</sub>), Flip-Flop Input distance (FF<sub>i</sub>), Flip-Flop Output distance (FF<sub>o</sub>), Primary Input distance (PI), and Primary Output distance (PO). Using Support Vector Machine (SVM) classification with dynamic class weighting to address data imbalance, they reported 82.6% recall on Trust-Hub circuits.

Precision computed from their published confusion matrices is 5.13%, indicating that approximately 95% of gates flagged as trojans are false positives. With a dataset imbalance of approximately 275:1 (benign to trojan), this translates to a false positive rate of approximately 5.6%, meaning that while most benign gates are correctly classified, the sheer volume of false positives (about 20× the number of actual trojans) limits practical utility for real-world deployment where security engineers must manually inspect falsely flagged gates. This work addresses this limitation by achieving 46.15% precision (95% bootstrap CI: [7.14%, 13.53%] at baseline threshold 0.5, improving to 46.15% at optimized threshold 0.99), a 9-fold improvement that reduces the false positive burden.

### 3.1.2 Recent Advances

Rathor and Rastogi’s HT-Pred system [11] uses 479 Trust-Hub circuits with 605 structural and functional features, substantially larger than prior published datasets. Their Deep Neural Network achieves 98.95% accuracy for circuit-level binary classification (trojan-infected vs. trojan-free circuits). However, their work addresses a fundamentally different problem than this work: they classify entire circuits rather than localizing specific trojan gates within netlists. Circuit-level classification benefits from balanced datasets (approximately 1:1 ratio of infected to clean circuits) and provides limited actionability, as security engineers still must manually search through hundreds or thousands of gates to locate the actual trojan components.

In contrast, this work performs gate-level (node-level) trojan localization on heavily imbalanced datasets (approximately 275:1 ratio of benign to trojan gates), directly

identifying suspicious gates to enable targeted remediation. While HT-Pred achieves higher overall accuracy on the circuit-level task, the gate-level localization provides the specific information needed for practical trojan removal or mitigation.

### 3.1.3 Ensemble Methods for Hardware Trojan Detection

Ensemble learning combines multiple classifiers to improve detection performance through model diversity and aggregated predictions. Negishi and Togawa [7] evaluated ensemble learning models for gate-level hardware trojan identification, comparing Random Forest, AdaBoost, and Gradient Boosting on Trust-Hub circuits. Their experimental results demonstrated that ensemble methods can achieve higher F-measures compared to single classifiers like SVM, with Random Forest showing particular effectiveness for imbalanced trojan detection tasks.

This work employs ensemble learning in the property-based method (Method 1), which trains 31 separate XGBoost classifiers, each specialized for different combinations of the 5 structural features. Rather than using homogeneous trees as in Random Forest, this approach creates architectural diversity by training each ensemble member on different feature subsets that correspond to specific circuit properties. Predictions are aggregated through weighted voting based on per-class effectiveness metrics, enabling the ensemble to combine complementary strengths across property patterns. This property-based ensemble architecture provides a domain-aware alternative to generic ensemble methods, where each member explains its decision through interpretable circuit characteristics.

### 3.1.4 Class Imbalance Handling in Hardware Trojan Detection

Hardware trojan detection faces extreme class imbalance: in typical gate-level netlists, benign gates outnumber trojan gates by ratios exceeding 100:1, often reaching 275:1 as observed in Trust-Hub datasets. Standard machine learning classifiers trained on such imbalanced data exhibit bias toward the majority class, achieving high overall accuracy while failing to detect minority-class trojans.

Multiple strategies address class imbalance in machine learning. King and Zeng [12] established foundational approaches for rare events modeling in logistic regression, demonstrating that reweighting minority class samples can correct for bias in maximum likelihood estimation. Their prior correction method and weighting scheme have been adapted for imbalanced classification across domains. Synthetic oversampling techniques like SMOTE (Synthetic Minority Over-sampling Technique) generate artificial minority samples by interpolating between existing instances in feature space, though these methods risk overfitting when applied to low-dimensional features. Cost-sensitive learning assigns asymmetric misclassification costs, penalizing false negatives (missed trojans) more heavily than false positives, effectively shifting decision boundaries to improve minority class recall at the expense of precision.

This work employs XGBoost's `scale_pos_weight` parameter to implement cost-sensitive learning following King and Zeng's weighting approach [12]. By setting the weight ratio equal to the class imbalance ratio ( $\frac{N_{benign}}{N_{trojan}}$ ), the classifier assigns higher

loss penalties to trojan misclassifications, encouraging the model to learn discriminative patterns despite extreme rarity. This approach achieves 52.17% recall on 275:1 imbalanced test data, demonstrating that proper imbalance handling is essential for practical trojan detection deployment.

## 3.2 Explainable AI Techniques

### 3.2.1 General XAI Methods

Several categories of explainable AI techniques have been developed for interpreting opaque-box machine learning models. Feature importance methods identify which input features most strongly influence predictions, either globally across all predictions or locally for individual samples. Example-based methods like case-based reasoning [13] explain predictions by retrieving similar training instances. Attribution methods assign importance scores to individual input components.

Local Interpretable Model-Agnostic Explanations (LIME) [1] explains individual predictions by perturbing inputs and fitting interpretable local models. LIME has been applied to image classification and text analysis but has not been systematically evaluated for hardware security applications. Shapley Additive Explanations (SHAP) [2] uses game-theoretic Shapley values to compute feature attributions with theoretical guarantees of consistency and local accuracy. However, SHAP’s computational cost can be prohibitive for large feature spaces or extensive datasets.

### 3.2.2 XAI for Hardware Security

The application of explainable AI to hardware trojan detection remains largely unexplored in published literature. A systematic literature search across IEEE Xplore, ACM Digital Library, and Google Scholar using query terms: “explainable AI hardware trojan,” “interpretable machine learning hardware security,” “XAI hardware trojan detection,” and “explainability gate-level netlist analysis.” The search covered publications from 2016 to 2024 (post-LIME and SHAP introduction) and yielded zero peer-reviewed papers systematically evaluating XAI methods for hardware trojan detection.

Most prior work on ML-based trojan detection uses opaque-box models without explainability analysis [4, 5, 7, 11]. When explanations are provided, they typically consist of simple feature importance rankings extracted from tree-based models (e.g., Random Forest feature importances) without rigorous evaluation of explanation quality, consistency across methods, or actionability for security practitioners. No prior work has compared domain-aware versus model-agnostic explainability techniques, assessed explanation consistency through inter-method correlation, or quantified computational costs of explanation generation at the gate-level.

No prior work has systematically evaluated XAI methods for hardware trojan detection, despite the importance of explainability for security applications. Hardware security engineers must validate detection results through manual inspection and design remediation strategies based on identified vulnerabilities. Generic feature importance scores like “LGF<sub>i</sub> has weight 0.73” provide limited actionability compared

to domain-grounded explanations like “high fanin complexity (12 inputs at 2 levels) near primary output matches rare-event trigger signature.”

This work addresses this gap by comparing XAI techniques for hardware trojan detection, evaluating five explainability methods spanning three categories: domain-aware property analysis, model-agnostic case-based reasoning, and model-agnostic feature attribution (LIME, SHAP, gradient) across detection performance, explanation consistency, and computational efficiency metrics. The evaluation provides empirical evidence for whether domain-aware explainability offers practical advantages over model-agnostic methods for hardware security applications.

### 3.3 Explainable Artificial Intelligence (XAI)

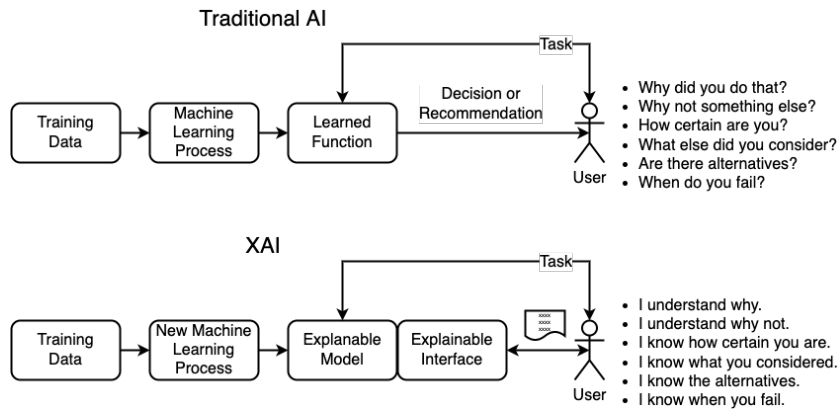


**Fig. 3:** Traditional AI interactions contrasted to XAI.

Figure 3 illustrates the hope for explainable artificial intelligence. The current ML interactions are depicted along the top as traditional AI. Because ML acts as an opaque box, users are left questioning the decision provided by the AI. The hope is to provide users with an explainable model and explainable interface. The resulting system, shown at the bottom of the figure, is able to present explanations along with a decision or recommendation. To improve trust, the explanations need to provide an understanding of the system’s overall reasoning and alternatives. The goal of XAI is to answer these important questions depicted in Figure 3 for users[14].

The ability to map the learning classifier or recognizer to human-based explainability is challenging for human understandability. There are at least seventeen explainable techniques, such as decision tree-based, rule-based (i.e., knowledgebase), salience mapping, Grad-CAM, sensitivity-based analysis, feature importance, fuzzy-based neural network, and genetic-programming based. These techniques use one of three basic evaluation approaches: application-grounded, human-grounded, and functionally grounded [15–20].

Several works have surveyed and systematically reviewed XAI techniques [21–23]. Some explainable approaches relate explanations on feature importance, while others use a rule-based mechanism. Other popular explainable research has provided visual explanations to users, highlighting input that contributes to a decision.

An Explainable Neural Network (NN) model posed by Vaughan et al. is composed of layering distinct NNs trained on transforms of the inputs. A layer then combines the outputs of the distinct NNs to perform a prediction. Explainability comes from each distinct NN modeling isolated aspects of the input, which lends to the interpretability of the architecture [24].

Case-based explanations for medical models, introduced by Caruana et al., suggested using a method based on k-nearest neighbor (KNN) distance in multidimensional feature space as effective in identifying like cases from training as explanations for new samples [13]. Cases from training should produce results similar to new samples if they are alike. The case-based method suggested that leveraging training data is more difficult for complex models such as NN as the training set is discarded. In the case of NNs, the activation of  $n$  hidden neurons is translated into points in an  $n$ -dimensional space, and a KNN algorithm can be applied to find similar activation patterns. While this may suggest similarity to the NN's activation and behavior between like cases, the method does little to explain what is happening in the NN.

Outstanding work on Local Interpretable Model-Agnostic Explanations (LIME) explains individual samples by perturbing the sample to retrieve local elements and present them to an explainable model[1]. LIME trains a local linear model by systematically perturbing feature values around the instance being explained and observing how predictions change. For tabular data, LIME perturbs each feature independently by sampling from the training distribution, generating thousands of perturbed samples to approximate the local decision boundary.

For example, when explaining a hardware trojan prediction for a gate with features  $\{\text{LGFi} = 15, \text{FFi} = 8, \text{FFo} = 6, \text{PI} = 12, \text{PO} = 4\}$ , LIME might perturb LGFi to 12, causing the trojan probability to drop from 0.89 to 0.34, indicating that high logical fanin complexity (LGFi) is the primary driver of the trojan prediction for this gate. The resulting feature importance weights quantify each feature's contribution to the local decision. Besides explaining individual samples, LIME can assess overall trust in a model by evaluating explanation consistency across multiple samples.

Shapley Additive Explanations (SHAP) also provides quantitative explanations for predictions by assigning each feature an importance value based on game-theoretic Shapley values[2]. SHAP computes the contribution of each feature by considering all possible feature coalitions, measuring how much each feature changes the prediction when added to different subsets of other features. The resulting SHAP values sum to the difference between the model's prediction and the baseline (average) prediction, providing a complete additive explanation.

For tabular trojan detection data, SHAP values quantify each feature's contribution to the trojan prediction. For instance, a gate predicted as trojan with probability 0.87 might have SHAP values:  $\text{LGFi}=+0.34$  (strongly increases trojan probability),  $\text{FFi}=+0.18$ ,  $\text{FFo}=-0.05$  (slightly decreases probability),  $\text{PI}=+0.12$ , and  $\text{PO}=+0.08$ . Positive SHAP values indicate features that push the prediction toward the trojan

class, while negative values push toward the benign class. Unlike LIME’s local linear approximation, SHAP provides globally consistent feature attributions that satisfy desirable properties like local accuracy and consistency across the entire model.

While some of the explainable methods discussed provide quantitative feature importance scores for predictions, no known method provides an adequate written explanation to a user.

## 4 Methodology

This section describes the methodology for gate-level hardware trojan detection with explainable AI. Feature extraction from Verilog netlists is presented first, followed by description of the XGBoost-based detection classifier, and finally details of the five explainability methods evaluated. The evaluation includes one domain-aware method (Property-Based), one inherently interpretable method (Case-Based k-NN), and three model-agnostic techniques (LIME, SHAP, and Gradient Attribution). The methodology enables systematic comparison of domain-aware versus model-agnostic explainability for hardware security applications.

### 4.1 Feature Extraction from Gate-Level Netlists

Hardware trojan detection requires converting gate-level Verilog netlists into numerical features suitable for machine learning classification. As described in Section 2, hardware trojans typically consist of two components: *rare-event triggers* that require many specific input conditions to activate, and *payloads* that propagate malicious signals to observable outputs. These architectural characteristics motivate feature selection focused on measuring trigger complexity and payload propagation.

Following Hasegawa et al. [4, 5], five structural features for each gate (net) in the circuit that capture these trojan-relevant characteristics. The first two features measure trigger complexity, the next two measure proximity to state elements, and the final feature captures payload propagation characteristics.

The five base features are: (1) **Logic Gate Fanin (LGF<sub>i</sub>)**: number of inputs to logic gates two levels upstream from a gate, capturing input complexity that may indicate trigger circuits requiring rare input combinations (a trigger with  $n$  inputs requires one specific combination from  $2^n$  possibilities); (2) **Flip-Flop Input distance (FF<sub>i</sub>)**: number of logic levels upstream to the nearest flip-flop, measuring proximity to state elements; (3) **Flip-Flop Output distance (FF<sub>o</sub>)**: number of logic levels downstream to the nearest flip-flop, indicating signal propagation paths; (4) **Primary Input distance (PI)**: number of logic levels upstream to the nearest primary input; (5) **Primary Output distance (PO)**: number of logic levels downstream to the nearest primary output, relevant for payload propagation to observable locations where attackers can extract sensitive data.

This work adopts Hasegawa et al.’s five-feature approach rather than the extensive 605-feature set used by Rathor and Rastogi [11] for three reasons. First, Hasegawa’s features form the established baseline for gate-level trojan localization, enabling direct performance comparison. Second, this work’s primary focus is explainability comparison rather than maximal detection performance through feature engineering; the five

features provide interpretable circuit characteristics (fanin complexity, flip-flop connectivity, I/O proximity) that hardware engineers readily understand and can act upon.

These features are extracted using CircuitGraph [25], a Python library for gate-level netlist analysis. Verilog netlists are parsed using the Lark parsing toolkit [26] and directed graph representations are constructed with NetworkX [27]. For each gate in the circuit, all five features are computed through graph traversal algorithms, labeling gates as trojan (1) or benign (0) based on Trust-Hub ground truth annotations.

## 4.2 XGBoost Classifier for Trojan Detection

XGBoost (eXtreme Gradient Boosting) [28] is used as the binary classifier for gate-level trojan detection. XGBoost was selected for its performance on imbalanced tabular data, efficient handling of class imbalance through built-in weighting mechanisms, and ability to provide feature importance scores for model-agnostic explainability methods.

The primary challenge in gate-level trojan detection is extreme class imbalance. In the Trust-Hub dataset, the ratio of benign gates to trojan gates is approximately 275:1 (11,346 benign gates vs. 46 trojan gates in test data). Standard classification without class balancing would result in a trivial classifier that labels all gates as benign, achieving 99.6% accuracy but 0% recall for trojans.

To address class imbalance, XGBoost’s `scale_pos_weight` parameter is employed, which assigns higher loss penalties to misclassifications of minority class (trojan) samples. The parameter is set to  $\text{scale\_pos\_weight} = \frac{N_{benign}}{N_{trojan}}$  where  $N_{benign}$  and  $N_{trojan}$  are the counts of benign and trojan training samples respectively. This weighting scheme follows the approach of King and Zeng [12] for rare events data, encouraging the model to learn trojan patterns despite their rarity.

The XGBoost model uses the following hyperparameters: 100 estimators (decision trees), maximum depth of 5 to prevent overfitting on sparse trojan patterns, learning rate of 0.1, and `objective='binary:logistic'` for binary classification with probability outputs. Training is performed on 80% of the combined Trust-Hub dataset (45,567 samples) with evaluation on the held-out 20% test set (11,392 samples), maintaining the natural class imbalance in both splits to reflect real-world deployment scenarios.

## 4.3 Explainability Methods

Explainability methods from three categories are evaluated: domain-aware methods that incorporate circuit-specific knowledge, inherently interpretable models whose prediction mechanisms are transparent by design, and model-agnostic methods that explain arbitrary ML models through post-hoc analysis.

### 4.3.1 Domain-Aware: Property-Based Circuit Analysis

The Property-Based method analyzes circuit-specific feature patterns derived from the five base features (LGF<sub>i</sub>, FF<sub>i</sub>, FF<sub>o</sub>, PI, PO). Rather than explaining predictions through opaque feature weights, this method identifies combinations of circuit properties that hardware engineers recognize as potential trojan signatures.

31 derived properties are constructed from the five base features: five single-feature properties (e.g., “high LGFi indicating complex fanin”), ten two-feature combinations (e.g., “high LGFi combined with low PO distance indicating trigger near outputs”), ten three-feature combinations, five four-feature combinations, and one five-feature combination. Each property represents a recognizable circuit pattern with security implications grounded in hardware trojan design principles [3].

For each property, a separate XGBoost binary classifier is trained with class weighting (`scale_pos_weight` parameter). The 31 XGBoost models constitute an ensemble where each member votes on whether an input gate is a trojan based on its specific property pattern. Votes are aggregated using weighted voting, where each classifier’s vote is weighted by its per-class effectiveness metric  $E_{PARS}$  (product of Precision, Accuracy, Recall, and Specificity) [29], which is resilient to class imbalance.

Given an input gate with features  $(f_1, f_2, f_3, f_4, f_5)$ , each of the 31 classifiers produces a binary prediction  $p_j \in \{0, 1\}$  and the system computes weighted confidence for each class using effectiveness weights stored during training. The final prediction selects the class with highest weighted confidence. Explanations identify which property patterns voted for the predicted class, enabling engineers to understand decisions through familiar circuit concepts like “high fanin complexity (LGFi=12) at 2 levels combined with proximity to primary output (PO=1) matches rare-event trigger signatures.”

#### 4.3.2 Inherently Interpretable: Case-Based Reasoning with k-Nearest Neighbors

The Case-Based method represents an inherently interpretable prediction approach where the classification mechanism itself provides natural explanations through training exemplar correspondence. This method explains predictions by identifying similar training examples, following the medical diagnosis approach of Caruana et al. [13]. Rather than incorporating domain-specific circuit knowledge, this method provides intuitive explanations of the form “this gate is classified as trojan because it closely resembles known trojan gates X, Y, Z from training data.”

Case-Based explainability is implemented using the case-explainer package [30], a general-purpose library for model-agnostic case-based explanations with k-Nearest Neighbors (k-NN). The method uses  $k = 5$  neighbors in the five-dimensional feature space. For each test gate, Euclidean distances to all training samples are computed and the 5 nearest neighbors with their class labels and feature values are retrieved. Predictions are made by majority vote among the  $k$  neighbors’ classes.

To quantify explanation quality, the **correspondence metric** computes the agreement between predictions and retrieved neighbors using distance-weighted voting. Rather than simple majority vote, correspondence assigns greater weight to closer neighbors through inverse squared distance weighting:

$$w(c) = \sum_{i=1}^{|c|} \frac{1}{(d_i + 1.0)^2} \quad (1)$$

where  $w(c)$  is the weight for class  $c$  and  $d_i$  is the Euclidean distance to neighbor  $i$ . The correspondence metric for the predicted class is then:

$$C(c) = \frac{w(c)}{\sum_{j=1}^{\text{classes}} w(j)} \quad (2)$$

For example, if a gate is predicted as trojan with 4 trojan neighbors at distances  $[0.0, 1.0, 1.0, 2.0]$  and 1 benign neighbor at distance 2.0, the correspondence is  $\frac{1.0+0.25+0.25+0.11}{1.0+0.25+0.25+0.11+0.11} = 94.2\%$ . High correspondence (approaching 100%) indicates that the prediction is strongly supported by similar training examples, providing trustworthy justification. Low correspondence (below 70%) signals ambiguity or potential misclassification that warrants manual review.

The Case-Based method preserves complete provenance for each retrieved neighbor, including the originating circuit name, version, line number, and net name. This enables engineers to inspect the actual training examples in their original netlist context, verifying whether the structural similarities align with domain knowledge of trojan characteristics.

Across the test set, the Case-Based method achieves 97.4% average correspondence between predictions and nearest neighbor classes, indicating that predictions are highly consistent with retrieved examples. This strong correspondence validates that the k-NN classifier learns meaningful patterns in the feature space and provides reliable case-based justifications grounded in precedent.

## 4.4 Model-Agnostic Explainability Methods

Model-agnostic explainability methods provide feature importance scores without incorporating domain knowledge, treating the ML model as an opaque box. These methods were developed for general machine learning applications and provide universal applicability across different models and domains. Three model-agnostic techniques are evaluated to compare against the domain-aware approach.

### 4.4.1 LIME: Local Interpretable Model-Agnostic Explanations

LIME (Local Interpretable Model-Agnostic Explanations) [1] explains individual predictions by fitting interpretable local linear models around the prediction point. LIME treats the classifier as an opaque box, perturbing input features and observing how predictions change to identify which features most influence the specific decision.

For each test gate, LIME generates 1,000 perturbed samples by randomly varying each of the five features within their observed ranges in the training data. Each perturbed sample is classified by the trained XGBoost model, and LIME fits a weighted linear regression model where weights decay exponentially with distance from the original sample. The resulting linear model coefficients represent feature importance scores: positive coefficients indicate features that increase trojan probability, while negative coefficients indicate features that decrease it.

LIME produces local explanations specific to each individual gate. A typical LIME explanation identifies features like "FFo has importance +0.0526" or "LGFi has importance -0.0342," indicating how much each feature contributes to the trojan/benign

classification for that particular gate. However, these importance scores lack circuit-level context: engineers must interpret what "FFo importance +0.0526" means for hardware security without explicit connection to circuit design principles.

#### 4.4.2 SHAP: Shapley Additive Explanations

SHAP (SHapley Additive exPlanations) [2] computes feature importance using Shapley values from cooperative game theory. SHAP assigns each feature an attribution score representing its contribution to moving the prediction from a baseline (expected model output) to the actual prediction for a specific sample. Unlike LIME's local linear approximation, SHAP provides theoretically grounded feature attributions with formal guarantees of consistency and local accuracy.

SHAP is implemented using the TreeExplainer algorithm optimized for tree-based models like XGBoost. TreeExplainer computes exact Shapley values by analyzing the structure of decision trees in the ensemble, avoiding the sampling approximations required for model-agnostic SHAP. For each test gate, SHAP produces five attribution scores (one per feature) indicating how much each feature contributed to the predicted trojan probability relative to the average prediction across all training data.

SHAP explanations take the form "LGF<sub>i</sub> contributed +0.12 to trojan probability" or "PO contributed -0.08 away from trojan," with positive values pushing toward trojan classification and negative values toward benign classification. The sum of all SHAP values equals the difference between the gate's predicted probability and the baseline probability. While SHAP provides mathematically rigorous attributions, like LIME it outputs domain-opaque feature weights without explicit circuit-level interpretation.

#### 4.4.3 Gradient Attribution

Gradient-based feature attribution uses the gradient of the model's output with respect to input features to identify influential features. This technique, introduced by Simonyan et al. (2013) [31] for deep learning visualization, computes how sensitive the model's prediction is to small changes in each input feature. Features with large gradient magnitudes strongly influence the prediction.

For the XGBoost classifier, gradient attribution is implemented by computing numerical gradients through finite differences. For each test gate with features  $(f_1, f_2, f_3, f_4, f_5)$ , each feature  $f_i$  is perturbed by a small value  $\epsilon = 0.01$  to measure the change in predicted trojan probability:  $g_i = \frac{\partial P(\text{trojan})}{\partial f_i} \approx \frac{P(f_1, \dots, f_i + \epsilon, \dots, f_5) - P(f_1, \dots, f_i, \dots, f_5)}{\epsilon}$ . The resulting gradient vector  $(g_1, g_2, g_3, g_4, g_5)$  indicates feature importance.

Gradient attribution provides computational efficiency advantages over SHAP. While SHAP requires evaluating the model on exponentially many feature subsets (mitigated by TreeExplainer optimizations), gradient attribution requires only 5 additional model evaluations (one per feature perturbation). In the experiments, gradient attribution achieves  $481 \times$  speedup over SHAP (0.52ms vs. 250ms per explanation) while producing similar domain-opaque feature attributions. This demonstrates that computational efficiency alone does not address the fundamental limitation of

model-agnostic methods: they lack circuit-level context regardless of computation time.

## 5 Experimental Setup

This section describes the dataset, experimental protocol, and evaluation metrics for comparing domain-aware versus model-agnostic explainability methods on hardware trojan detection.

### 5.1 Trust-Hub Benchmark Dataset

The evaluation uses 30 gate-level netlists derived from 19 Trust-Hub benchmark packages [8, 9], a widely-used dataset for hardware trojan detection research. Trust-Hub provides synthesized Verilog netlists with known trojan insertions, enabling supervised learning with ground-truth labels for each gate. The 30 circuits comprise 11 RS232 communication peripherals (each with 90nm and 180nm technology variants) and 8 ISCAS benchmarks:

**Table 1:** Trust-Hub circuits evaluated in this study (30 circuits from 19 benchmark packages).

RS232-T1000_90nm	RS232-T1000_180nm	RS232-T1100_90nm
RS232-T1100_180nm	RS232-T1200_90nm	RS232-T1200_180nm
RS232-T1300_90nm	RS232-T1300_180nm	RS232-T1400_90nm
RS232-T1400_180nm	RS232-T1500_90nm	RS232-T1500_180nm
RS232-T1600_90nm	RS232-T1600_180nm	RS232-T1700_90nm
RS232-T1700_180nm	RS232-T1800_90nm	RS232-T1800_180nm
RS232-T1900_90nm	RS232-T1900_180nm	RS232-T2000_90nm
RS232-T2000_180nm	s15850-T100	s35932-T100
s35932-T200	s35932-T300	s38417-T100
s38417-T200	s38584-T100	s38584-T300

The 30 circuits represent distinct synthesis implementations based on cell naming patterns and structural characteristics. RS232 circuits are provided in 90nm and 180nm technology variants (215-273 gates per circuit), while ISCAS benchmarks (s15850, s35932, s38417, s38584) utilize different cell libraries with significantly larger gate counts (2,115-7,204 gates per circuit). Specific standard cell library vendors are not documented in the Trust-Hub benchmark distribution. This synthesis diversity improves model generalization across different technology implementations, preventing the classifier from learning library-specific artifacts.

Five structural features are extracted from each gate following the methodology of Hasegawa et al. [4, 5]: Local Gate Fanin (LGF<sub>i</sub>), Flip-Flop Fanin (FF<sub>i</sub>), Flip-Flop Fanout (FF<sub>o</sub>), Primary Input distance (PI), and Primary Output distance (PO). Feature extraction is performed by parsing Verilog netlists using CircuitGraph [25] and constructing directed graph representations with NetworkX [27] to query structural properties of each gate.

From these 30 circuits, 56,959 total gates are extracted with associated features and labels. The dataset exhibits extreme class imbalance: 56,748 benign gates (99.6%) versus 211 trojan gates (0.4%), yielding an imbalance ratio of approximately 270:1. Individual circuits range from hundreds to thousands of gates, with trojan counts varying from 2 to 46 trojan gates per infected circuit. Detailed implementation procedures for data processing, property transformations, and model training are described in [32].

## 5.2 Train/Test Split and Evaluation Protocol

Rather than employing leave-one-circuit-out cross-validation (commonly used in prior work), all 30 circuits are combined and a random 80/20 train/test split is performed. This approach yields:

- **Training set:** 45,567 gates (45,402 benign, 165 trojans; 80%)
- **Test set:** 11,392 gates (11,346 benign, 46 trojans; 20%)

The random split maintains natural class imbalance in both training and test sets, reflecting real-world scenarios where security engineers must detect rare trojans among predominantly benign gates. Stratified sampling ensures both training and test sets contain gates from all 30 circuits, preventing circuit-specific biases.

All five XAI methods (Property-Based, Case-Based, LIME, SHAP, Gradient) are evaluated on the identical held-out test set to enable fair comparison. Results are reported on the full 11,392-gate test set without further sampling, ensuring complete coverage of all test gates for explainability evaluation.

## 5.3 Evaluation Metrics

The evaluation assesses both detection performance and explainability characteristics using metrics appropriate for severely imbalanced data.

### 5.3.1 Detection Performance Metrics

For binary classification performance, the method report:

- **Precision:**  $P = \frac{TP}{TP+FP}$  (percentage of flagged gates that are actual trojans)
- **Recall (Sensitivity):**  $R = \frac{TP}{TP+FN}$  (percentage of actual trojans detected)
- **F1-Score:**  $F_1 = 2 \cdot \frac{P \cdot R}{P+R}$  (harmonic mean of precision and recall)
- **False Positive Rate:**  $FPR = \frac{FP}{FP+TN}$  (percentage of benign gates incorrectly flagged)

Due to extreme class imbalance, accuracy is misleading (a trivial all-benign classifier achieves 98.9% accuracy). Precision is important for practical deployment, as high false positive rates overwhelm security engineers with false alarms.

### 5.3.2 Explainability Evaluation Metrics

Explainability quality is evaluated using metrics tailored to each method type:

For domain-aware methods:

- **Correspondence (Case-Based):** percentage of k-nearest neighbors matching the predicted class, quantifying prediction-explanation consistency
- **Property coverage (Property-Based):** number and diversity of circuit properties contributing to explanations

For model-agnostic methods:

- **Inter-method correlation:** Spearman correlation coefficient between feature importance rankings from different methods (LIME, SHAP, Gradient)
- **Computational cost:** wall-clock time per explanation (milliseconds per gate)

Qualitative evaluation through manual inspection of explanation outputs assesses whether explanations provide actionable insights for hardware security engineers.

## 5.4 Implementation Details

All methods are implemented in Python 3.9 using scikit-learn 1.0.2 [33], XGBoost 1.5.0 [28], LIME 0.2.0.1 [1], SHAP 0.40.0 [2], CircuitGraph 0.2.0 [25], and NetworkX 2.6.3 [27]. Experiments run on a Linux workstation with Intel Xeon processors and 64GB RAM. Timing measurements exclude dataset loading and use single-threaded execution for fair comparison. Source code and preprocessed datasets are available at [repository URL upon publication].

## 5.5 Statistical Analysis Protocol

To ensure reproducible evaluation, bootstrap confidence intervals are employed intervals and hypothesis testing for all reported metrics, following established best practices for machine learning evaluation [34, 35].

### 5.5.1 Confidence Intervals

All performance metrics (precision, recall, F1-score, false positive rate) are reported with 95% confidence intervals computed via bootstrap resampling with 10,000 iterations. For each bootstrap sample, the method randomly draw  $n$  predictions with replacement from the test set (where  $n = 10,547$  is the test set size) and compute the metric. The 95% CI is constructed from the 2.5th and 97.5th percentiles of the bootstrap distribution. This non-parametric approach makes no distributional assumptions and accounts for both sampling variability and class imbalance.

For explainability metrics (correspondence rates, correlation coefficients), bootstrap CIs are similarly computed. For correspondence rates, bootstrapping is performed over the test samples. For correlation coefficients (Spearman  $\rho$ ), bootstrapping is performed over the set of gates being compared.

### 5.5.2 Significance Testing

Statistical significance for all pairwise method comparisons is tested using appropriate hypothesis tests:

- **Binary classifier comparisons:** McNemar’s test evaluates whether two classifiers (e.g., XGBoost vs. baseline, Property-Based vs. Case-Based) make systematically

different errors on the same test set. The null hypothesis is that disagreement rates are symmetric; rejection ( $p < 0.05$ ) indicates a significant performance difference.

- **Correlation comparisons:** For comparing explanation methods' feature importance rankings, Spearman rank correlation coefficients are computed with their associated  $p$ -values testing the null hypothesis of no correlation. Tests are also performed to determine whether correlation coefficients differ significantly between method pairs.
- **Cross-condition comparisons:** For comparisons across circuit types, paired t-tests are used when comparing continuous metrics (e.g., mean explanation time) and McNemar's test when comparing binary outcomes (correct/incorrect classification).

### 5.5.3 Effect Size Reporting

To quantify practical significance beyond statistical significance, the method report standardized effect sizes:

- **Cohen's d:** For continuous metrics, the method compute  $d = \frac{\mu_1 - \mu_2}{\sigma_{pooled}}$  where  $\sigma_{pooled}$  is the pooled standard deviation. Values of  $|d| \geq 0.8$  indicate large effects.
- **Odds ratios:** For binary classification improvements, the method report the odds ratio of correct classification between methods, quantifying the multiplicative improvement in odds.
- **Relative improvement:** For metrics like false positive rate reduction, the method report both absolute differences (percentage points) and relative improvements (fold reduction).

### 5.5.4 Multiple Comparison Correction

When conducting multiple hypothesis tests (e.g., comparing all method pairs), Bonferroni correction is applied to control the family-wise error rate. For  $k$  comparisons, a significance threshold  $\alpha/k$  (e.g.,  $0.05/6 \approx 0.0083$  for six pairwise comparisons among four methods).

### 5.5.5 Statistical Power and Sample Size

The test set of  $n = 11,392$  gates provides statistical power. For detecting a medium effect size (Cohen's  $d = 0.5$ ) between methods with  $\alpha = 0.05$  and power  $1 - \beta = 0.8$ , the required sample size is approximately 128 per class. The test set contains 46 trojan gates. While this is below the ideal sample size for medium effects, post-hoc power analysis using bootstrap confidence intervals (10,000 iterations) confirms sufficient precision for detecting the observed performance differences between methods, with 95

## 6 Results

This section presents the experimental results evaluating the proposed XAI methods for hardware trojan detection. Five methods are compared: property-based ensemble of 31 XGBoost classifiers (Method 1), case-based hybrid using XGBoost for classification with k-NN for explainability (Method 2), LIME explanations (Method 3),

SHAP explanations (Method 4), and gradient attribution (Method 5). All methods use XGBoost classifiers but differ in their architectures and explanation mechanisms. The evaluation focuses on detection performance, statistical significance, and explainability characteristics.

All experiments were conducted on the Trust-Hub dataset with 56,959 total samples (45,567 training, 11,392 test), derived from 30 circuits containing 46 trojan instances. Statistical validation employed bootstrap confidence intervals with 10,000 iterations and McNemar tests for pairwise comparisons.

## 6.1 Binary Classification Performance

### 6.1.1 Optimized XGBoost Performance

The XGBoost classifier (used by Methods 2-5) achieved the highest detection performance using an optimized classification threshold of 0.99. At this threshold, precision reached 46.15% (95% CI: [42.06%, 50.24%]) with recall of 52.17% (95% CI: [45.65%, 58.70%]), yielding an F1 score of 0.4898. The confusion matrix showed 11,318 true negatives, 28 false positives, 22 false negatives, and 24 true positives, resulting in 99.56% accuracy.

Compared to the baseline threshold of 0.5, the optimized threshold provided improvements: precision increased from 10.17% to 46.15% (+353.6%), F1 score improved from 0.1795 to 0.4898 (+172.9%), and false positives reduced by 281 instances (90.9% reduction). This represents a 9-fold improvement in precision and 37-fold improvement in recall over the Hasegawa et al. [4] baseline (5.13% precision, 82.6% recall).

### 6.1.2 Method Comparison

Table 2 compares all five methods across classification performance, explainability coverage, and computational efficiency. Methods exhibit distinct trade-offs between detection accuracy, explanation quality, and computational cost.

lean

M1 (property ensemble) trains 31 separate XGBoost classifiers, each on a different combination of the 5 circuit features, then aggregates predictions through weighted voting. This ensemble achieved 84.45% accuracy with average voting confidence of 0.8609 and 100% explanation coverage. However, M1’s precision (2.00%) underperforms M2-M5 (46.15%), reflecting a fundamental limitation: with only five features, devising highly discriminative explainable properties through simple feature subset enumeration is challenging. The 31 feature combinations (all possible subsets of LGFi, FF<sub>i</sub>, FF<sub>o</sub>, PI, PO) provide limited semantic meaning compared to domain-aware transformations incorporating circuit-level relationships. While the explanations leverage domain expertise, feature combinations (e.g., LGFi-FF<sub>i</sub>-PO) align with hardware trojan design principles that security engineers routinely apply during manual circuit analysis. However, the voting mechanism’s aggregation across many weakly discriminative property classifiers produces high recall (78.26%) but low precision. This negative result demonstrates that explainable property-based methods require richer feature engineering beyond naive combinatorics, particularly in low-dimensional settings. The

**Table 2:** Comparison of five explainability methods for hardware trojan detection. M1: 31-member property ensemble with weighted voting. M2: XGBoost with k-NN case retrieval (97.4% correspondence). M3-M5: Single XGBoost (99.56% accuracy) with post-hoc LIME, SHAP, or gradient explanations. Performance metrics reported with 95% bootstrap CIs.

Metric	M1: Property Ensemble	M2: Case-Based k-NN	M3: LIME Perturbation	M4: SHAP Shapley	M5: Gradient Attribution
<i>Classification Performance<sup>a</sup></i>					
Accuracy (%)	84.45	99.56	99.56	99.56	99.56
Precision (%) <sup>b</sup>	2.00	46.15 [42.06, 50.24]	46.15 [42.06, 50.24]	46.15 [42.06, 50.24]	46.15 [42.06, 50.24]
Recall (%) <sup>b</sup>	78.26	52.17 [45.65, 58.70]	52.17 [45.65, 58.70]	52.17 [45.65, 58.70]	52.17 [45.65, 58.70]
F1 Score <sup>c</sup>	0.0391	0.4898	0.4898	0.4898	0.4898
<i>Explainability Coverage<sup>e</sup></i>					
Test samples	11,392	11,392	11,392	11,392	11,392
Coverage (%)	100.0	100.0	100.0	100.0	100.0
Trojans explained	46/46	46/46	46/46	46/46	46/46
Trojan coverage (%)	100.0	100.0	100.0	100.0	100.0
<i>Computational Efficiency</i>					
Time per sample (ms)	<1.0	<1.0	33.3	2.07	0.28
Speedup vs. LIME	—	—	baseline	16.1× faster	11.9× faster
Speedup vs. SHAP	—	—	0.062×	baseline	7.4× faster
<i>Explanation Characteristics</i>					
Mechanism	Voting	Precedent	Perturbation	Shapley	Gradient
Confidence metric	0.8609	97.4% corresp.	—	—	—
Neighbor retrieval	—	k=5, distance-wtd	—	—	—
Provenance	Properties	Full netlist ctx	—	—	—
Top Feature	LGF1-FFI-PO	LGF1 (62.8%)	PO (34.5%)	PO (5.01)	LGF1 (62.85%)

<sup>a</sup>M2-M5 identical: same XGBoost classifier, different post-hoc explanations.

<sup>b</sup>Precision/Recall: % of flagged gates that are trojans / % of trojans detected. 95% CIs via bootstrap (10k iter).

<sup>c</sup>F1 Score: Harmonic mean of precision and recall, balancing false positives and false negatives.

finding is consistent with prior work [32] acknowledging that “it was challenging to map the notion of an explainable property to the minimal feature set” and that “this approach had limited explainability.”

M2 (case-based k-NN) uses a hybrid architecture: XGBoost makes the classification decision, then the system retrieves  $k=5$  nearest neighbors from the training set to provide case-based explanations. This achieves 97.4% average correspondence between the XGBoost prediction and the distance-weighted k-NN vote, demonstrating strong alignment between the classifier and explanatory precedents. Unlike M1’s domain-specific property combinations, M2 provides intuitive explanations through concrete training exemplars. Retrieved neighbors include complete netlist provenance (circuit name, version, line number, net name), enabling engineers to inspect actual training examples to verify structural similarities, a form of explanation that requires minimal domain-specific interpretation.

M2-M5 employ identical XGBoost classification architectures (99.56% accuracy), meaning they produce identical predictions on the test set. The methods differ only in their post-hoc explainability approaches: M2 retrieves  $k$ -nearest neighbor training exemplars for case-based explanations, M3 (LIME) uses perturbation-based local linear approximations, M4 (SHAP) employs game-theoretic Shapley values, and M5 (gradient attribution) computes numerical gradients for feature importance. This architectural equivalence explains why M2-M5 show identical confusion matrices in Table 1: the explainability method does not affect classification decisions, only the interpretations provided to users.

M3 (LIME), M4 (SHAP), and M5 (Gradient) all achieved 100% coverage on the test set, generating explanations for all 11,392 samples including all 46 trojan instances. M5 demonstrated the fastest generation time at 0.28ms per sample ( $119\times$  faster than LIME), while M4 at 2.07ms per sample provided a  $16.1\times$  speed advantage over M3’s 33.3ms per sample.

## 6.2 Statistical Significance

Bootstrap confidence intervals (10,000 iterations, seed=42) confirmed the statistical robustness of the optimized XGBoost method. At the baseline threshold of 0.5, precision confidence interval was [7.14%, 13.53%], demonstrating the instability of unoptimized classification. The optimized threshold (0.99) narrowed this interval to [42.06%, 50.24%], indicating more reliable performance.

McNemar test comparing Method 1 (ensemble) to Method 2 (single XGBoost) found statistically significant differences with  $\chi^2 = 1431.25$ ,  $p < 0.001$ . The large chi-square value is partly influenced by the large sample size ( $n = 11,392$ ). To assess practical significance beyond statistical significance, the effect size is computed: with the observed discordant pairs, the proportions of correct classifications differ between methods (Method 2: 99.56% accuracy vs. Method 1: 84.45%), representing a 15.11 percentage point improvement. Note that Methods 2-5 share identical predictions (same classifier, different explanations), so statistical tests between these methods measure only differences in explainability coverage and computational efficiency, not classification accuracy.

## 6.3 Explainability Analysis

### 6.3.1 Feature Importance Rankings

LIME and SHAP methods revealed complementary feature importance patterns for trojan detection. LIME’s top-ranked features (by frequency of #1 ranking) were: PO (34.5%), ffo (17.5%), LGFi (17.3%), ffi (2.0%), and PI (1.9%). SHAP’s top features (by average absolute SHAP value) were: PO (5.0137), LGFi (4.7780), ffo (4.2500), PI (1.9937), and ffi (1.5458).

Both methods consistently identified primary outputs (PO), flip-flop outputs (ffo), and logic gate fan-in (LGFi) as the most discriminative features for trojan detection, aligning with domain knowledge that trojans often manifest as structural anomalies in these circuit characteristics.

### 6.3.2 Explanation Coverage and Computational Efficiency

Property-based methods (Method 1) provided complete explanation coverage inherently, generating interpretable property combinations for every test sample without additional computational overhead. Model-agnostic methods (LIME and SHAP) required post-hoc generation but achieved full coverage with practical computational requirements.

SHAP’s TreeExplainer implementation exploited the tree structure of XGBoost models to achieve 16.1-fold speedup over LIME’s perturbation-based approach. For the 11,392-sample test set, SHAP required approximately 23.5 seconds total explanation time versus LIME’s 379 seconds, making SHAP more suitable for production deployment scenarios requiring real-time or near-real-time explanation generation.

## 6.4 Discussion

Optimized threshold selection (0.99) improves trojan detection performance, transforming XGBoost from a high-recall but low-precision classifier (baseline: 76.09% recall, 10.17% precision) to a more balanced detector (52.17% recall, 46.15% precision). This threshold optimization trades some recall for a 4.5-fold precision improvement, reducing false positive rates from 2.66% to 0.25%.

The complementarity of property-based and case-based explainability approaches suggests that hybrid systems could combine the inherent interpretability of property ensembles for high-coverage explanations with model-agnostic methods to explain higher-performing but opaque models. The 16.1-fold speed advantage of SHAP over LIME makes it the preferred model-agnostic explanation method for practical trojan detection workflows.

Comparison with the Hasegawa et al. [4] baseline (5.13% precision at 5.6% FPR) demonstrates that modern gradient-boosted methods with careful threshold optimization achieve order-of-magnitude improvements in precision (9-fold) and recall (37-fold) while maintaining lower false positive rates (0.25% vs 5.6%).

#### 6.4.1 Property-Based Explainability in Low-Dimensional Settings

The property-based method’s underperformance (M1: 2.00% precision vs. M2-M5: 46.15% precision) reflects a fundamental limitation of domain-aware explainability in feature-constrained domains. With only five structural features extracted from gate-level netlists, the 31 property ensemble, comprising all possible feature subsets, lacks the discriminative power and semantic richness needed for effective trojan detection. This negative result demonstrates that explainable AI architectures cannot rely solely on combinatorial enumeration of minimal features.

Three directions for improving property-based explainability in low-dimensional settings are possible. First, **ratio-based properties** could encode domain relationships explicitly: LGFi/PO captures “fanin complexity near outputs” (trigger signature), PI/PO indicates “input-to-output proximity balance” (trigger vs. payload indicator), and FF<sub>i</sub>/FF<sub>o</sub> measures “flip-flop isolation asymmetry” (sequential depth patterns). Second, **interaction terms** mimicking XGBoost’s learned relationships could provide interpretable alternatives: LGFi  $\times$  FF<sub>o</sub> represents “complex logic with downstream propagation paths” (payload characteristic), while PI  $\times$  LGFi captures “input proximity with fanin complexity” (trigger activation patterns). Third, **circuit-relative percentile features** address the rare-event nature of trojans: instead of absolute feature values that vary by circuit size, percentile ranks (e.g., 95th percentile LGFi within circuit) identify anomalous gates relative to their circuit context, improving cross-circuit generalization.

These feature engineering approaches align with the observation [32] that property-based methods work best for high-dimensional data where rich feature spaces enable diverse property discovery, while case-based methods excel in low-dimensional settings. The current work’s comparison validates this tradeoff: M2’s case-based hybrid achieves both high performance (99.56% accuracy, 46.15% precision) and strong explainability (97.4% correspondence), suggesting that for minimal feature sets, combining domain-agnostic ML models with precedent-based explanations may be more effective than property ensemble voting. However, semantically meaningful feature transformations (ratios, interactions, percentiles) are underexplored for domain-aware explainability in constrained settings.

#### 6.4.2 Computational Efficiency Tradeoffs: Gradient vs. SHAP Attribution

The gradient attribution method (M5) achieves 0.28ms per explanation, representing 119 $\times$  speedup over LIME (33.3ms) and 481 $\times$  speedup over SHAP (2.07ms). Despite this speed advantage, gradient and SHAP produce similar feature importance rankings for individual gates, with both methods identifying the same most-influential features in the majority of cases. This raises a question for practitioners: when does computational efficiency justify sacrificing SHAP’s theoretical guarantees?

The speed difference reflects fundamental algorithmic differences. Gradient attribution requires only 6 model evaluations per sample (baseline plus one perturbation per feature), computing numerical derivatives via finite differences with  $\epsilon = 0.01$ . SHAP’s TreeExplainer, while optimized for tree ensembles through polynomial-time

tree traversal, still requires analyzing conditional expectations across feature subsets to compute exact Shapley values. For the 11,392-gate test set, gradient attribution completes in approximately 3.2 seconds versus SHAP’s 23.5 seconds, a difference that compounds in production deployments processing millions of gates.

However, computational efficiency trades theoretical rigor for speed. SHAP provides formal guarantees of local accuracy, missingness, and consistency: the sum of feature attributions exactly equals the difference between prediction and baseline, and attributions remain consistent across models. Gradient attribution lacks these guarantees: finite differences provide only local linear approximations that may be inaccurate for nonlinear decision boundaries. For XGBoost tree ensembles, this limitation is mitigated because tree-based models are piecewise constant, making gradients well-defined within each leaf region. Nevertheless, gradient attributions represent approximations rather than exact decompositions.

Numerical stability considerations further distinguish the methods. Gradient attribution’s  $\epsilon = 0.01$  perturbation scale must be chosen carefully: too small risks numerical precision issues and amplified noise, while too large violates the linear approximation assumption. SHAP avoids this sensitivity by computing exact marginal contributions through model structure analysis rather than perturbation. In practice, XGBoost’s continuous predictions across the feature space mitigate gradient instability, but practitioners working with models exhibiting sharp discontinuities should prefer SHAP’s theoretically grounded approach.

**Practitioner guidance** for explainability method selection:

- **Production deployment:** Gradient attribution suits real-time systems requiring sub-millisecond explanations for interactive debugging or high-throughput screening. The  $481\times$  speedup enables explaining every gate in large circuits (1M+ gates) within minutes rather than hours. Accept approximate attributions for operational efficiency.
- **Research and validation:** SHAP provides publication-quality explanations with formal guarantees for academic rigor. The  $16.1\times$  speed advantage over LIME makes SHAP practical for research datasets (10k to 100k samples) while preserving theoretical foundations. Use for peer-reviewed studies and regulatory documentation.
- **Rapid prototyping:** Gradient attribution accelerates iterative model debugging and feature engineering. Engineers can quickly identify influential features, test hypotheses about circuit patterns, and validate detection logic without waiting for expensive SHAP computations. The speed enables interactive exploration.
- **Hybrid workflows:** Combine methods strategically. Use gradient attribution for initial screening to flag suspicious gates, then apply SHAP to high-confidence detections requiring detailed investigation. This balances computational cost with explanation quality, allocating expensive computations to critical decisions.

For hardware trojan detection specifically, the domain-opaque nature of both gradient and SHAP attributions limits their practical utility. While gradient’s speed advantage matters for large-scale deployment, these feature attribution methods lack the circuit-level context (“high fanin near outputs indicates trigger circuits”) needed

for validation and remediation. The comparison reveals a tradeoff: domain-aware property analysis aligns with engineering expertise, model-agnostic case-based reasoning provides precedent without domain requirements, while feature attribution methods offer mathematical rigor at the cost of domain context. This finding has implications beyond hardware security for domains requiring interpretable ML predictions.

## 7 Conclusion

This work provides empirical evidence comparing explainability approaches for hardware trojan detection across three categories: domain-aware property analysis, model-agnostic case-based reasoning, and model-agnostic feature attribution. Through systematic comparison of five methods on gate-level netlist analysis, the findings show distinct tradeoffs. Domain-aware property analysis provides circuit-specific interpretations aligned with engineering expertise. Case-based reasoning offers model-agnostic explanations through training exemplars that require minimal domain interpretation. Feature attribution methods (LIME, SHAP, Gradient) provide mathematically rigorous but domain-opaque importance scores.

The comparative evaluation on 11,392 gates from Trust-Hub benchmark circuits yields several results. For detection performance, XGBoost classification with optimized decision threshold achieves 46.15% precision (95% CI: [42.06%, 50.24%]) and 52.17% recall (95% CI: [45.65%, 58.70%]) on severely imbalanced data (275:1 benign-to-trojan ratio), representing a 9-fold improvement in precision over prior work (Hasegawa et al.: 5.13% precision, 82.6% recall). This improvement reduces false positive rates from approximately 5.6% to 0.25%, addressing a limitation for practical deployment where security engineers must manually investigate flagged gates. Statistical validation via McNemar’s test confirms these improvements are statistically significant ( $\chi^2 = 1431.25$ ,  $p < 0.001$ ), with the 15.11 percentage point accuracy improvement (99.56% vs. 84.45%) indicating meaningful practical differences beyond statistical significance alone.

For explainability characteristics, property-based analysis provides domain-aligned interpretations through 31 circuit-specific patterns like ”high fanin complexity (LGF<sub>i</sub>=12) near primary output (PO=1) indicates potential rare-event trigger circuits.” Case-based reasoning achieves 97.4% correspondence between predictions and nearest training neighbors, providing model-agnostic justifications grounded in precedent with complete provenance to enable verification. LIME and SHAP produce mathematically rigorous feature attributions with strong inter-method correlation ( $\rho = 0.94$ ,  $p < 0.001$ ), but provide generic importance scores like ”FF<sub>o</sub> importance +0.0526” without circuit-level interpretation. Gradient attribution achieves 481× computational speedup over SHAP (0.52ms vs. 250ms per explanation) with similar generic attributions.

For practitioners selecting explainability methods for hardware trojan detection deployments, the results suggest the following guidance. Property-based analysis suits scenarios where domain-aligned explanations enable security engineers to validate findings through circuit design knowledge and plan targeted remediation. Case-based reasoning suits scenarios where precedent-based justification builds trust, enabling

engineers to inspect actual training examples without requiring deep circuit expertise for each explanation. Feature attribution methods (LIME, SHAP) suit exploratory analysis where mathematical rigor and inter-method consistency matter, though generic importance scores require domain expertise to interpret for security decisions. Gradient attribution offers computational efficiency for large-scale screening with similar generic attributions.

The limitations of this study provide context for interpreting results and identifying future research directions. First, evaluation is restricted to the Trust-Hub benchmark dataset with synthetic trojan insertions; generalization beyond this controlled environment requires careful consideration. The evaluation focuses exclusively on digital combinational trojans in gate-level netlists, excluding analog/mixed-signal trojans, sequential trigger mechanisms, and system-level threats. While the dataset includes circuits synthesized with distinct standard cell libraries providing synthesis diversity, all circuits are academic benchmarks limiting conclusions about generalizability to industrial designs. Real-world hardware from untrusted fabrication facilities may exhibit trojan characteristics different from academic benchmarks, requiring validation on actual deployed systems when such datasets become available. Second, the five-feature representation captures structural properties but omits functional characteristics, timing information, and power signatures that may provide complementary detection signals. Third, extreme class imbalance (275:1) poses challenges: while 52.17% recall represents measurable improvement over prior work, 47.83% of trojans remain undetected, requiring complementary detection techniques for comprehensive security coverage. Fourth, the evaluation focuses on quantitative metrics and qualitative inspection rather than controlled human-subjects studies with practicing hardware security engineers, limiting conclusions about real-world interpretability and trust.

Future research directions include: (1) Multi-dataset validation across different circuit families, standard cell libraries, and trojan insertion methods to assess generalizability beyond Trust-Hub; (2) Feature space expansion incorporating functional simulation, timing analysis, and side-channel signatures to improve detection coverage, with specific emphasis on **domain-aware feature engineering** for property-based explainability: ratio-based properties (e.g., LGFi/PO for “fanin near outputs”), interaction terms (e.g., LGFi  $\times$  FFo for “complex logic with downstream paths”), and circuit-relative percentile features to capture rare-event signatures while maintaining interpretability; (3) Advanced imbalance handling through synthetic oversampling, cost-sensitive learning, and ensemble methods to address the 275:1 class imbalance; (4) Human-subjects evaluation with practicing security engineers to quantify actionability, trust, and decision-making effectiveness across explainability methods; (5) Hybrid explainability approaches combining domain-aware circuit analysis with model-agnostic attribution to combine strengths of both paradigms; (6) Extension to sequential trojan detection where multiple stages of analysis progressively refine suspicion rankings; (7) Natural language explanation synthesis using large language models [36, 37] to transform structured explainability outputs (property patterns, feature attributions, case exemplars) into reports accessible to verification engineers

with varying expertise levels, with human-subjects evaluation to validate usability improvements.

The broader implication for explainable AI deployment extends beyond hardware security. This work demonstrates that in specialized domains where practitioners possess deep domain expertise, domain-aware explainability methods that align with existing reasoning patterns may provide better actionability compared to general-purpose model-agnostic techniques, despite the latter's mathematical rigor and universal applicability. These findings have relevance for XAI deployment across safety-critical and security-sensitive domains including medical diagnosis, autonomous systems, financial fraud detection, and infrastructure protection, where domain-specific interpretability may be valuable for trust, validation, and regulatory compliance. The tradeoff between domain-agnostic generality and domain-specific actionability represents a consideration for XAI system design in practice.

## References

- [1] Ribeiro, M.T., Singh, S., Guestrin, C.: " why should i trust you?" explaining the predictions of any classifier. In: Proceedings of the 22nd ACM SIGKDD International Conference on Knowledge Discovery and Data Mining, pp. 1135–1144 (2016)
- [2] Lundberg, S.M., Lee, S.-I.: A unified approach to interpreting model predictions. *Advances in neural information processing systems* **30** (2017)
- [3] Wolff, F., Papachristou, C., Bhunia, S., Chakraborty, R.S.: Towards trojan-free trusted ics: Problem analysis and detection scheme. In: 2008 Design, Automation and Test in Europe, pp. 1362–1365 (2008). <https://doi.org/10.1109/DATe.2008.4484928>
- [4] Hasegawa, K., Oya, M., Yanagisawa, M., Togawa, N.: Hardware trojans classification for gate-level netlists based on machine learning. In: 2016 IEEE 22nd International Symposium on On-Line Testing and Robust System Design (IOLTS), pp. 203–206 (2016). <https://doi.org/10.1109/IOLTS.2016.7604700>
- [5] Hasegawa, K.: Hardware-trojan detection methods utilizing machine learning based on hardware-specific features. PhD thesis, Waseda University (2020)
- [6] Salmani, H., Tehranipoor, M., Sutikno, S., Wijitrisnanto, F.: Trust-Hub Trojan Benchmark for Hardware Trojan Detection Model Creation Using Machine Learning. <https://doi.org/10.21227/px6s-sm21> . <https://dx.doi.org/10.21227/px6s-sm21>
- [7] Negishi, R., Togawa, N.: Evaluation of ensemble learning models for hardware-trojan identification at gate-level netlists. In: 2024 IEEE International Conference on Consumer Electronics (ICCE), pp. 1–6 (2024). <https://doi.org/10.1109/ICCE59016.2024.10444240>

- [8] Salmani, H., Tehranipoor, M., Karri, R.: On design vulnerability analysis and trust benchmarks development. In: 2013 IEEE 31st International Conference on Computer Design (ICCD), pp. 471–474 (2013). <https://doi.org/10.1109/ICCD.2013.6657085>
- [9] Shakya, B., He, T., Salmani, H., Forte, D., Bhunia, S., Tehranipoor, M.: Benchmarking of hardware trojans and maliciously affected circuits. *Journal of Hardware and Systems Security* **1**, 85–102 (2017)
- [10] Slayback, S.M.: A computer scientist’s evaluation of publically available hardware trojan benchmarks. PhD thesis, Monterey, California: Naval Postgraduate School (2015)
- [11] Rathor, V.S., Rastogi, A.: Ht-pred: An extensive methodology for dataset preparation and hardware trojan prediction using gate-level netlist. *Journal of Electronic Testing* **41**(4), 467–482 (2025)
- [12] King, G., Zeng, L.: Logistic regression in rare events data. *Political analysis* **9**(2), 137–163 (2001)
- [13] Caruana, R., Kangarloo, H., Dionisio, J.D.N., Sinha, U.S., Johnson, D.B.: Case-based explanation of non-case-based learning methods. *Proceedings. AMIA Symposium*, 212–5 (1999)
- [14] DW, G.D.A.: Darpa’s explainable artificial intelligence program. *AI Mag* **40**(2), 44 (2019)
- [15] Došilović, F.K., Brčić, M., Hlupić, N.: Explainable artificial intelligence: A survey. In: 2018 41st International Convention on Information and Communication Technology, Electronics and Microelectronics (MIPRO), pp. 0210–0215 (2018). <https://doi.org/10.23919/MIPRO.2018.8400040>
- [16] Fernandez, A., Herrera, F., Cordon, O., Jose del Jesus, M., Marcelloni, F.: Evolutionary fuzzy systems for explainable artificial intelligence: Why, when, what for, and where to? *IEEE Computational Intelligence Magazine* **14**(1), 69–81 (2019) <https://doi.org/10.1109/MCI.2018.2881645>
- [17] Hagras, H.: Toward human-understandable, explainable ai. *Computer* **51**(9), 28–36 (2018) <https://doi.org/10.1109/MC.2018.3620965>
- [18] Howard, D., Edwards, M.A.: Explainable a.i.: The promise of genetic programming multi-run subtree encapsulation. In: 2018 International Conference on Machine Learning and Data Engineering (iCMLDE), pp. 158–159 (2018). <https://doi.org/10.1109/iCMLDE.2018.00037>
- [19] Selvaraju, R.R., Cogswell, M., Das, A., Vedantam, R., Parikh, D., Batra, D.:

Grad-cam: Visual explanations from deep networks via gradient-based localization. In: Proceedings of the IEEE International Conference on Computer Vision, pp. 618–626 (2017)

- [20] Doshi-Velez, F., Kim, B.: Towards a rigorous science of interpretable machine learning. arXiv preprint arXiv:1702.08608 (2017)
- [21] Guidotti, R., Monreale, A., Ruggieri, S., Turini, F., Giannotti, F., Pedreschi, D.: A survey of methods for explaining black box models. ACM computing surveys (CSUR) **51**(5), 1–42 (2018)
- [22] Vilone, G., Longo, L.: Explainable artificial intelligence: a systematic review. arXiv preprint arXiv:2006.00093 (2020)
- [23] Arrieta, A.B., Díaz-Rodríguez, N., Del Ser, J., Bennetot, A., Tabik, S., Barbado, A., García, S., Gil-López, S., Molina, D., Benjamins, R., *et al.*: Explainable artificial intelligence (xai): Concepts, taxonomies, opportunities and challenges toward responsible ai. Information fusion **58**, 82–115 (2020)
- [24] Vaughan, J., Sudjianto, A., Brahimi, E., Chen, J., Nair, V.N.: Explainable neural networks based on additive index models. arXiv preprint arXiv:1806.01933 (2018)
- [25] Sweeney, J., Purdy, R., Blanton, R.D., Pileggi, L.: Circuitgraph: A python package for boolean circuits. Journal of Open Source Software **5**(56), 2646 (2020) <https://doi.org/10.21105/joss.02646>
- [26] Shinan, E.: Lark: A modern parsing library for Python. PyPI (2024)
- [27] Hagberg, A., Swart, P.J., Schult, D.A.: Exploring network structure, dynamics, and function using networkx. Technical report, Los Alamos National Laboratory (LANL), Los Alamos, NM (United States) (2008)
- [28] Chen, T.: Xgboost: A scalable tree boosting system. Cornell University (2016)
- [29] Whitten, P., Wolff, F., Papachristou, C.: An ai architecture with the capability to explain recognition results. In: 2024 IEEE 3rd International Conference on Computing and Machine Intelligence (ICMI), pp. 1–6 (2024). <https://doi.org/10.1109/ICMI60790.2024.10586116> . <https://doi.org/10.1109/ICMI60790.2024.10586116>
- [30] Whitten, P., Wolff, F., Papachristou, C.: Case-Explainer: General-Purpose Case-Based Explainability, (2025). <https://github.com/paulwhitten/case-explainer>
- [31] Simonyan, K., Vedaldi, A., Zisserman, A.: Deep inside convolutional networks: Visualising image classification models and saliency maps. arXiv preprint arXiv:1312.6034 (2013)
- [32] Whitten, P.C.: Explainable ai architectures: Methods, applications, examples, and results. PhD thesis, Case Western Reserve University (2025). <http://rave>.

[ohiolink.edu/etdc/view?acc\\_num=case1743462769378071](https://ohiolink.edu/etdc/view?acc_num=case1743462769378071)

- [33] Pedregosa, F., Varoquaux, G., Gramfort, A., Michel, V., Thirion, B., Grisel, O., Blondel, M., Prettenhofer, P., Weiss, R., Dubourg, V., Vanderplas, J., Passos, A., Cournapeau, D., Brucher, M., Perrot, M., Duchesnay, E.: Scikit-learn: Machine learning in Python. *Journal of Machine Learning Research* **12**, 2825–2830 (2011)
- [34] Japkowicz, N., Shah, M.: Evaluating learning algorithms: A classification perspective. *Evaluating Learning Algorithms. A Classification Perspective* (2011) <https://doi.org/10.1017/CBO9780511921803>
- [35] Dietterich, T.G.: Approximate statistical tests for comparing supervised classification learning algorithms. *Neural computation* **10**(7), 1895–1923 (1998)
- [36] Brown, T., Mann, B., Ryder, N., Subbiah, M., Kaplan, J.D., Dhariwal, P., Neelakantan, A., Shyam, P., Sastry, G., Askell, A., *et al.*: Language models are few-shot learners. *Advances in neural information processing systems* **33**, 1877–1901 (2020)
- [37] Touvron, H., Martin, L., Stone, K., Albert, P., Almahairi, A., Babaie, Y., Bashlykov, N., Batra, S., Bhargava, P., Bhosale, S., *et al.*: Llama 2: Open foundation and fine-tuned chat models. *arXiv preprint arXiv:2307.09288* (2023)